PHILOSOPHICAL
TRANSACTIONS A

Phil. Trans. R. Soc. A.
doi:10.1098/not yet assigned

Diagnosing oceanic nutrient deficiency

C. Mark Moore

Ocean and Earth Science, National Oceanography Centre Southampton, University of Southampton,
European Way, Southampton SO14 3ZH UK

Keywords: Nutrients, trace metals, ocean biogeochemistry

Summary

The supply of a range of nutrient elements to surface waters is an important driver of oceanic production and the subsequent linked cycling of the nutrients and carbon. Relative deficiencies of different nutrients with respect to biological requirements, within both surface and internal water masses, can be both a key indicator and driver of the potential for these nutrients to become limiting for the production of new organic material in the upper ocean. The availability of high quality, full depth and global scale data sets on the concentrations of a wide range of both macro- and micro- nutrients produced through the international GEOTRACES programme provides the potential for estimation of multi-element deficiencies at unprecedented scales. Resultant coherent large scale patterns in diagnosed deficiency can be linked to the interacting physical-chemical-biological processes which drive upper ocean nutrient biogeochemistry. Calculations of ranked deficiencies across multiple elements further highlight important remaining uncertainties in the stoichiometric plasticity of nutrient ratios within oceanic microbial systems and caveats with regards to linkages to upper ocean nutrient limitation.

Main Text

Introduction

The uptake of nutrients involved in the production of new organic matter by planktonic microbes in the upper-ocean, combined with the subsequent export and remineralisation of this material within the ocean interior, has a profound influence on the oceanic cycling of a range of nutrient elements (1-3). When combined with the associated carbon fluxes, this cycling of organic matter production, export and remineralisation constitutes the biological carbon pump (BCP) (4), which acts to store a large amount of dissolved inorganic carbon in the deep ocean and exerts a major control on atmospheric pCO_2 (5-7). Simultaneously, the availability and supply of a range of nutrients to the upper ocean frequently exerts a fundamental constraint on the rate (8) and/or absolute (9) production of new organic matter in the surface layer (10, 11). Reciprocal interactions between internal oceanic nutrient cycling and upper ocean microbial activity are hence a key driver of global biogeochemical processes (12). In particular, nutrient limitation can set a fundamental constraint on the local strength and overall efficiency of the BCP (10, 11, 13).

Establishing where, when and how certain nutrients come to be limiting in the upper ocean represents a key challenge for our understanding of the Earth system (11, 13) alongside the behaviour of this system over a range of timescales (14, 15). The extent of this challenge is only emphasised through ongoing recognition that, alongside the so-called macronutrients (N, P and Si), the oceanic cycling of many of the trace metal elements (e.g. Fe, Mn, Zn, Ni, Cu, Co, Cd) is profoundly influenced by biological processes, while some may also have the potential to reciprocally influence upper ocean microbiological processes (11, 12, 16). Indeed, despite the long hiatus between the earliest suggestions that Fe limitation may be an important process in oceanic systems and development of the analytical techniques which made

---

*Author for correspondence (cmm297@noc.soton.ac.uk).
†Present address: Ocean and Earth Science, National Oceanography Centre Southampton, University of Southampton, European Way, Southampton SO14 3ZH UK

rigorous investigation of this problem possible (17), the potential for trace metal (co-)limitation of phytoplankton productivity is now firmly established (11, 18-20). The advent of the high quality global scale data sets which are emerging as a result of the international GEOTRACES project (21) promises to be further transformative in our understanding of the linked biogeochemical cycles of multiple nutrients in oceanic systems.

Defining deficiency

Although sometimes conflated, the concepts of nutrient limitation and nutrient deficiency are distinct (11). Here previous usage (11, 22) will be adopted, whereby limitation refers to a situation where either the (bio-)availability of a given nutrient is limiting for the rate of production of new biomass (8) or the overall supply of a given nutrient is setting a limit on the overall biomass (9). The significance of any distinction between such so called 'rate' (8) or 'yield' (9) type limitations respectively will be explicitly acknowledged where relevant in the context of what follows. However, it is worth noting that the two concepts may frequently be linked (19). For example, the overall biomass of a community would not be expected to respond to an increased supply of a limiting nutrient unless the production of some component of the community were previously rate limited by the availability of that nutrient (11). Moreover it is important to recognise that development of nutrient limitation and the characteristics of a nutrient limited system are emergent properties of the reciprocal feedbacks which occur between microbes and nutrients (12). For example, within simple conceptual models (23, 24), which appear to have reasonable predictive skill in the oceans (25, 26), the standing stock of microbial biomass will be a function of the supply rate of the limiting nutrient and not the concentration of this nutrient (27). Simultaneously, biological uptake would be expected to set the equilibrium nutrient concentration at a subsistence level which will be a function of the ecosystem properties and independent of the nutrient supply rate (23, 24, 27).

The deficiency of one nutrient element relative to another is closely related to concepts of ecological stoichiometry (28, 29), which have been fundamental in developing our understanding of marine biogeochemical nutrient cycling (1, 30). The seminal works of Redfield (1, 30), revealed both the importance of stoichiometry in linking the biogeochemical cycles of the different nutrient elements (and carbon) and the potential for consideration of biological and dissolved chemical stoichiometric ratios (Figure 1) as a means of understanding oceanic biogeochemistry. Such ideas are exemplified by the classical 'Redfield ratio' of C_{106}: N_{16}:P_1, which is assumed to reflect some average ratio of the three elements within oceanic primary producers or, more broadly, within the multiple components and transformations of the BCP. Consequently, assuming the elemental ratios of the different nutrients within a microbial cell are known, a nutrient can be considered deficient within the extracellular environment if the concentration or supply of this nutrient is low relative to all the others (11, 19). Thus, for example, two different water masses having dissolved N:P ratios of 20:1 and 14:1, i.e. above or below an assumed 16:1 ratio respectively, might be considered deficient in P and N respectively (31).

Nutrient deficiency can thus be considered as indicative of the potential for ('Liebig type' (9)) nutrient limitation to develop (19). Within a strictly stoichiometrically conserved system, i.e. where the uptake and cycling of every nutrient always occurs in a fixed ratio, the nutrient which is most deficient might be expected to be the first to become limiting (9). However, this only happens once microbial uptake has depleted this nutrient. Moreover, again within a stoichiometrically conserved system, once limitation by the most deficient nutrient develops, the other nutrients would be expected to remain replete (9, 26). However, such arguments can break down once the potential for flexibility in the stoichiometric coupling of different nutrient cycles is acknowledged (11, 19, 29, 32).

In addition to the microbial community influencing the availability of nutrients, in many circumstances it may be important to distinguish between deficiency of nutrient availability/concentration within a volume of seawater and the deficiency of overall supply (26). The overall ratios of nutrient supply to a region of the ocean surface can be decoupled from concentration ratios in source waters by additional external sources, including from the atmosphere or continental margin/sediment interactions (33-36). Thus, although nutrient deficiency may be linked to the potential for limitation, it cannot be taken as a sufficient condition for limitation at that particular time and location (11). For example, relative deficiencies of different nutrients within sub-surface waters of the global ocean may be estimated through comparing assumed biological requirements with the concentrations of the dissolved species of these elements (Figure 1). However, there is little evidence that nutrient availability is directly limiting microbial processes in the sub-surface. Rather, any understanding of the relative deficiencies of nutrients in the ocean interior can potentially inform our understanding of how patterns of nutrient limitation emerge in the near surface (37), where the nutrients resupplied through physical transport become depleted through the net production of new organic matter.

Quantifying deficiency

Previous studies of large scale variability in nutrient deficiency, alongside the causes and consequences of these patterns, have often utilised linear combinations of the measured concentrations of 2 nutrients related through their known (or assumed) ratio within biological material (3, 31, 37-39). Such combined tracers, typically denoted by a '*' notation, have been used for investigating a range of processes relating to nutrient cycling including: N* and P* as tracers for N_2 fixation and denitrification (31, 38, 40, 41), Si* as a measure of the preferential removal of Si relative to N within the Southern Ocean (SO) and a tracer of subsequent global scale transport of SO sourced waters (39) and Fe* as a tracer of the decoupling of Fe and P in the ocean (37). Calculation of such tracers can be visualised and the derived values related to a more general consideration of the relative biological requirements and availability of multiple nutrients (Figure 2). Indeed, for any pair of nutrients, X and Y, a generalised notation could be adopted whereby:

$$X_Y^* = X_{dissolved} - R_{X:Y} Y_{dissolved} \qquad \text{Eqn. 1}$$

where $R_{X:Y}$ represents the measured or assumed ratio of the two nutrients in newly formed (and/or remineralised) organic matter. Such a generalised notation can be mapped onto past usage e.g. N_P* (38), Si_N* (39), Fe_P* (37), P_N* (31), Cd_P* (42), Zn_{Si}* (43), noting that the later two usages differ as the assumed ratios are derived from observed correlations between the two nutrients within the ocean interior, rather than an assumed biological uptake ratio.

The use of linear combinations of two nutrients has significant advantages over ratios, due to the mathematically tractable behaviour of such a 'quasi-conservative' tracer on water mass mixing as opposed to the highly non-linear behaviour of ratios (38, 41). Moreover, assuming the ratio ($R_{X:Y}$) is fully conserved by some process within the biogeochemical system, such linear combinations can in principal provide quantitative information on other processes which do not conserve this ratio (31, 38) alongside tracing the large scale imprint of such processes (39). However, within the specific context of multi-element nutrient deficiency, it would rapidly become challenging to consider all of the multiple combinations which could be calculated simultaneously within any given seawater volume (Figure 2). For example, 28 combinations could be derived from simply considering the 8 nutrients at least as deficient as Si within the water mass considered in Figure 2. Moreover, with the exception of the macronutrients (N, P and Si), until recently (21) there has been a lack of high quality multi-nutrient data sets with which to undertake a broader analysis.

The marked stoichiometric plasticity (i.e. variable values for $R_{X:Y}$) which can be observed in cultures of marine phytoplankton (12, 44), as well as within marine organic matter and the biogeochemical imprints of some BCP related processes (44-47), further complicates the interpretation of combined tracers (X_Y*). Stoichiometric plasticity is particularly acute for the trace metals due to non-specific uptake (12, 48-51) and so called 'luxury' uptake (52, 53), alongside multiple mechanisms for reducing quotas under conditions where a nutrient becomes limiting, including the use of metabolically substitutable alternate nutrient elements (19, 54). Consequently use of Fe_P*, for example, has largely been limited to that of a diagnostic tracer within models where the biological stoichiometry is fixed at an assumed value (37). Even for the macronutrients N and P, it has become apparent that observed significant variability in $R_{N:P}$ (45) needs to be taken into account when both evaluating the mechanisms responsible for generating patterns of N_P* (P_N*) in the ocean and understanding the associated biogeochemical processes (41, 55-57). Indeed, observations of upper ocean organic material (45) and the apparent remineralisation ratios of this material (46, 47) are revealing how large scale variations in biological stoichiometry are likely a key component of oceanic biogeochemical cycles.

In contrast to considering quantitative linear combinations (X_Y*), estimates of relative nutrient deficiency can also be derived through simply comparing measured concentrations within a given seawater volume to assumed overall stoichiometric biological requirements (11, 19). For example, the nutrient which is furthest towards the bottom right corner (as presented) in Figures 1 and 2 would be estimated to be the most deficient. This calculation is equivalent to finding the nutrient *X'* for which a normalised quantity X'_Y* (Eqn. 1) is the most negative for all *Y* (Figure 2). Previous work using conceptually similar calculations outline the associated caveats that need to be considered (11, 19). In particular, alongside aforementioned stoichiometric flexibility, issues concerning variable bioavailability of different nutrient species need to be considered (11, 19). Use of such analyses to derive quantitative information on the relative deficiency of different nutrients may thus be premature. However, using conservative assumptions it may still be possible to obtain qualitative information on the relative deficiencies of multiple nutrient elements and hence potentially derive insight into certain aspects of the controls on upper ocean nutrient limitation. Until recently, it was only possible to perform such analyses in a global average or limited regional sense (11). Release of the GEOTRACES intermediate data product (21) makes it timely to revisit such considerations.

Methods

The international GEOTRACES programme is producing unprecedented measurements of multiple trace elements at full oceanic depth across ocean-basin to global scales (21, 58, 59). Public release of this data in the form of the consistent quality controlled (60) GEOTRACES Intermediate Data Product (IDP) 2014 (21) has provided a hugely valuable community resource which promises to revolutionise our understanding of the sources, sinks and cycling of trace elements, alongside their interactions with oceanic microbial systems and wider biogeochemical cycles. Here the IDP2014 is used to derive large scale patterns in relative nutrient deficiency of multiple nutrient elements.

Data on the distributions of the macronutrient elements N, P, Si (43, 61-66), the micronutrient elements Fe, Mn, Ni, Zn and Cd (63, 67-83) and the non-nutrient element Al (66, 84, 85) were downloaded from the IDP2014 collection (21) and imported into a MATLAB™ environment for analysis. For each sampling location and/or seawater volume/water mass, a ranking of the relative deficiencies of multiple nutrient elements was calculated by dividing observed dissolved concentrations by an assumed 'typical' stoichiometric ratio within newly formed organic (biological) material (Figure 1) (11, 19). Dissolved seawater concentrations and biological stoichiometeries were both initially normalised to N. Although useful for calculation and visualisation (e.g. Figure 2), such normalisation makes no difference to the subsequent ranking of relative deficiencies. For each nutrient (X_i), the derived value of the observed dissolved concentration [X_i] normalised to [N] and the assumed biological ratio ($R_{Xi:N}$) was thus:

$$X_i' = \frac{[X_i]}{[N]R_{X_i:N}} \qquad \text{Eqn. 2}$$

The nutrient with the minimum value of this derived quantity is then the most deficient. A full ranking of relative deficiencies of all the observed and chosen nutrients can similarly be calculated.

Derived relative deficiencies crucially depend on the assumed values for $R_{Xi:N}$, which, as discussed above, are expected to vary as a complex function of both the species of microbe (typically phytoplankton) responsible for the initial production of new organic matter (44, 86), as well as the availability of the nutrient in question, in some cases alongside the availability of other nutrients and other external environmental factors (11, 12). Initially, the same 'typical' value is adopted as previously (11), which in turn was largely derived on the basis of a previously published average across multiple phytoplankton taxa (86). Thus the range of $R_{Xi:N}$ initially adopted corresponds to an 'extended Redfield formula' (86) of:

$$(C_{7.75}N_1Si_1P_{0.0625})_{1000}Fe_{0.469}Mn_{0.175}Ni_{0.0625}Zn_{0.05}Cd_{0.013}$$

In many cases this 'typical' stoichiometry appears broadly consistent with independently observed correlations between the different dissolved nutrients and/or apparent oxygen utilisation in the upper ocean, measurements of oceanic particulate organic matter and direct measurements on individual cells within natural phytoplankton communities (44). However, these cellular ratios for Mn and Fe appear to be substantially (around 10 fold) higher than alternative observations and estimates within the oceans (44), likely due to choices made regarding metal concentrations in the media. Consequently a sensitivity analysis is performed whereby repeated calculations are carried out assuming that cellular Fe and Mn quotas for newly formed organic matter in the ocean are, on average, an order of magnitude lower, i.e. the corresponding extended Redfield formula would be:

$$(C_{7.75}N_1Si_1P_{0.0625})_{1000}Fe_{0.0469}Mn_{0.0175}Ni_{0.0625}Zn_{0.05}Cd_{0.013}$$

Calculations were also performed in a sequential manner leaving out certain nutrients. Inferences from such sensitivity analyses and significant remaining caveats associated with the plasticity of phytoplankton elemental stoichiometry are revisited below.

An idealised model (25, 26, 87) is also utilised to illustrate the expected qualitative outcome of interactions between 3 key nutrients, N, P and Fe and two broadly defined types of organism, a non-diazotrophic primary producer and a diazotrophic primary producer. The latter organisms are assumed to have a higher requirement for Fe as a result of the high abundance of this element within the nitrogenase enzyme which catalyses N_2 fixation (88, 89). The basic model is essentially identical to that described previously (87). In the current context the model was run across a range of initial starting conditions, corresponding to variable sub-surface supply ratios of N:P:Fe and a range of imposed external Fe supplies (26). System interactions then result in a series of equilibrium states which vary across the imposed gradient of external Fe supply. Specifically, the system switches between a high macronutrient, Fe limited condition, then two different categories of states where the non-diazotrophs are N limited and the diaztrophs are limited by P or Fe, see (26) for full analytical treatment and discussion.

Results and Discussion

Patterns of deficiency 1: N, P and Fe

Initial calculations are performed for the elements N, P and Fe. In addition to major components of the cellular metabolic requirements for these elements being absolute and irreducible, there is considerable evidence that all play some role in in dictating patterns of upper ocean nutrient limitation (11). Within nutrient limited regions of the ocean, microbial activity would be expected to have depleted the limiting nutrient to an equilibrium subsistence concentration, while other non-limiting nutrients remain replete (24, 26, 27). Consequently, within surface waters a first order relationship might be expected between direct experimental evidence of nutrient limitation, as for example derived on the basis of observed biological responses within *in vitro* or *in situ* nutrient enrichment experiments (18, 20) and calculations of nutrient deficiency on the basis of dissolved concentrations. A previous compilation of experimental evidence (11), reveals clear first order patterning of the surface ocean into predominantly N limited low latitude (sub-)tropical surface waters and Fe limited high latitude and upwelling regions (Figure 3a). Derivation of the most deficient nutrient between N, P and Fe in surface waters (<30m depth) on the basis of the IDP2014 data set (Figure 3b) reveals a very similar spatial pattern (Figure 3b), which is reasonably robust to assumptions concerning variability in the Fe:N(:P) ratio (Figure 4 a-c).

The observed correspondence between experimental evidence of nutrient limitation (Figure 3a) and calculated deficiency on the basis of dissolved concentrations and an assumed biological stoichiometry (Figure 3b) supports a first order conceptual understanding of the system (11), while highlighting the potential utility of the GEOTRACES data set in a biological context. However, the result itself is perhaps unsurprising, given that surface water N concentrations span >3 orders of magnitude between low latitude oligotrophic systems and the high nitrate waters of the SO, while observed surface water Fe concentrations typically vary by ~<2 orders of magnitude, presumably at least partially reflecting the influence of buffering by organic complexation (90, 91). Indeed, available experimental evidence of Fe limitation can be largely mapped onto those regions of the ocean where residual nitrate is observed at the surface (11).

Performing the same calculation on a full depth basis for the IDP2014 reveals how deficiency of Fe compared to N and P predominates throughout the subsurface ocean (Figure 4 d-f). A meridional section through the Atlantic compiled using data across the multiple GEOTRACES cruises within the IDP2014 provides a useful illustration (Figure 5). With the exception the hydrothermal plume from the TAG vent site sampled at around 3300m at 26°N on GEOTRACES line GA03 (78), Fe deficiency is estimated below 200m depth throughout this section. In contrast, N (and/or P) deficiency is only observed above the main thermocline (and associated nitracline), within the N depleted near surface waters of the oligotrophic North and South Atlantic (sub-)tropics from ~40°S to ~40°N (Figure 5). Within the majority of these near surface waters N appears deficient relative to P. Upper nutricline waters within the North Atlantic Sub-tropical Gyre (NASG), which are well known to be characterised by an excess of N relative to P with reference to the canonical Redfield ratio (i.e. a positive N_P* value relative to an $R_{N:P}$ of 16:1) are a clear exception, likely resulting from cumulative influence of net N_2 fixation (38) as a result of the relief of Fe limitation of N_2 fixation within the dust fertilised surface waters of the North Atlantic gyre (87, 92, 93).

Implications of the Fe deficiency of the sub-surface ocean

The observed sub-surface deficiency of Fe relative to N (and P) is driven by the high particle reactivity of Fe (94) resulting in adsorption to sinking particles and hence loss from the dissolved phase to scavenging (91, 95). Consequently, while surface production, export and sub-surface remineralisation of organic material delivers N, P and Fe to the interior, scavenging acts to remove Fe, strongly decoupling the sub-surface cycling of these nutrients (37). In addition to providing confirmation of the ubiquity of subsurface Fe deficiency within the ocean, results from the performed simple analysis can be further considered in the context of physical processes which return interior waters to the productive surface (Figure 5). Thus, in the absence of other local/regional sources/factors, such as interactions with sediments on the continental shelves (34, 35), dust deposition (33), or specific sub-surface conditions including marked oxygen minima (83), any upwelled or upwardly mixed waters are likely to be deficient in Fe throughout the majority of the oceans. Development of Fe limitation in ~30% of the surface waters of the open ocean (11, 20), should hence perhaps not be surprising. Indeed, depletion of bioavailable N and associated development of N limitation within the vast low latitude oligotrophic regions (11) presumably requires an additional external source of Fe. Within the highly stratified (sub-)tropics, low rates of (Fe-deficient) sub-surface nutrient resupply and the long residence times of warm buoyant waters at the surface likely contributes to the depletion of N being possible even for those regions where atmospheric (33) or other Fe inputs are relatively low. A clear low latitude exception is the Eastern Sub-tropical Pacific, where upwelling is strong and Fe limitation develops (96, 97).

In the context of the large scale overturning circulation of the Atlantic, the performed analysis suggests that both the major sources of deep water to the global ocean, North Atlantic Deep Water (NADW) and Antarctic Bottom Water (AABW) may already be deficient in Fe at the point of subduction (Figure 5). Although such a conclusion is close to being sensitive to the choice of $R_{Fe:N}$ within reasonable bounds for NADW (Figure 4e & 7a). Such deficiency presumably reflects the predominance of surface water Fe deficiency (Figure 3b) and the associated Fe limited status of surface waters, at least seasonally (98), within both generation regions (Figure 3a). At global scale, the resupply of deep waters and the nutrients they contain to the surface ocean is dominated by upwelling in the SO (39, 99). Deficiency of Fe within these upwelled waters (Figures 1, 4f & 5), will thus be a key driver of Fe limitation in the SO (100). Moreover, although sub-surface supply likely dominates the overall surface Fe budget of the SO (101), this supply is always expected to be deficient in Fe. Hence strong upwelling acts to maintain Fe deficiency (Figure 3b) and Fe limitation (Figure 3a) in the surface SO (7). Past alterations in the nutrient status and BCP efficiency of the SO thus needs to be considered in the context of the strength of Fe deficient sub-surface nutrient resupply, alongside the potential for enhanced non-internal Fe sources from dust (15).

Removal of sub-surface Fe by scavenging is expected to produce residence times which are short relative to oceanic circulation timescales (16, 91, 94). However, recent evidence, particularly from hydrothermal vent plumes (102-104), suggests that subsurface transport of Fe may still occur over significant distances, presumably due to some processes stabilising deep ocean Fe concentrations (105). Such large scale transport of persistent deeply sourced Fe (104,

106) will act to reduce the overall magnitude of subsurface Fe deficiency (Figure 4 e, f & 5) and likely contributes significantly to sustaining production following deep water upwelling in the SO (104).

Secondary deficiency: feedbacks and external inputs

In addition to estimating the primary (1°) deficient nutrient, similar calculations can be performed to calculate the secondary (2°) deficient nutrient. Partitioning of surface waters into 1° Fe deficient high latitude regions and N deficient low latitude systems (Figure 3) appears to be related to the primary limitation of the bulk phytoplankton communities living in these waters (11). Organisms capable of fixing N_2, diazotrophs, would be expected to have a selective advantage within the low latitude N deficient regions, but may subsequently become limited by other nutrients such as P and Fe (93, 107, 108). Taking into account the potential for external sources of Fe to supplement internal fluxes, alongside subsequent feedbacks as diazotrophs utilise available P and Fe in providing additional of N to the system, a conceptually simple model can illustrate the expected emergent steady state properties of such a system (25, 26). Specifically, given a general deficiency of N relative to P (i.e. negative N*) in upwelled waters (38, 41), the system is expected to transition between a series of distinct states as external inputs of Fe increase. In the oceanic context these states will correspond to provinces going from: i) high N (and P), Fe deficient and Fe limited systems at low Fe:N input ratios, through to N deficient (and N limited for non-diazotrophs) systems where initially there is, ii) high P and low Fe (and Fe limited diazotrophs) before a final transition to iii) low P, high Fe conditions (and P limited diazotrophs) at highest overall Fe:P input ratios (26). The distinct provinces within such a system should thus be characterised by switches between: i) 1° Fe deficiency and 2° N deficiency, ii) 1° N deficiency and 2° Fe deficiency and finally, iii) 1° N deficiency and 2° P deficiency (26), as can be illustrated using an idealised model (Figure 6 a, c).

Within the Atlantic Ocean, where gradients in external Fe sources to the open ocean surface are likely dominated by atmospheric dust deposition (33, 93, 109), this conceptual model appears to have reasonable predictive skill in describing observed large scale concentrations of the nutrients N, P and Fe, alongside the biogeography of diazotrophs (25, 26). Transitions between the different regimes (i-iii) might thus be expected to occur along a gradient in atmospheric dust input as, for example, inferred using surface distributions of a non-nutrient tracer such as Al (85). Examining the distributions of Al, N, P and Fe from the IDP2014 in this conceptual context reveals a first order qualitative agreement between the expected and observed inter-relationships between these dissolved constituents (Figure 6). Consequently, in addition to revealing large scale patterns of 1° nutrient deficiency (Figures 3 & 4), even in the absence of any corresponding biological data, the IDP2014 appears to allow new tests of existing hypotheses concerning the more complex interactions expected within an idealised 3 nutrient 2 organism system (26).

Deficiency beyond N, P and Fe: Mn and Zn

Consideration of relative deficiencies within a wider range of potential (co-)limiting nutrients rapidly becomes more complicated (Figure 4). Despite many of the conclusions above being reasonably robust to a potential order of magnitude overestimate within initially adopted values for the biological Fe:N(P) ratios (Figure 4, Figure 7a), recognition of the full physiological potential for stoichiometric flexibility in these ratios (Figure 1) complicates the picture when considering other metals in low abundance relative to biological requirements. For example, thermocline waters of the NASG are characterised by potential deficiency in multiple trace metals relative to N and P. Given uncertainties related to variable stoichiometry alongside associated biochemical substitutions (12, 19), developing a robust ordering for their relative deficiency is difficult. However, recognising these caveats, some interesting general patterns can still be discerned from consideration of a wider, albeit still limited subset of the nutrients (Figure 7).

Phytoplankton have an absolute requirement for the micronutrient Mn, in part due to the presence of this element within the water splitting complex (16, 28, 44). There is some direct (110, 111) and indirect (112, 113) evidence for the (co-)limiting potential of Mn within oceanic surface waters. Calculating the relative deficiency of both Fe and Mn relative to N and P (Figure 7 c & d) reveals that Fe largely remains the most deficient nutrient at high latitudes within the upper ocean (~<200m). However, there are a few locations within the SO surface where Mn may be at least as deficient as Fe with respect to the assumed ranges of biological stoichiometry (Figure 7c). Moreover, Mn is estimated to be the 2° deficient nutrient within the surface SO (Figure 7d) and is almost as deficient as Fe within the subsurface SO, as illustrated through consideration of CDW (Figure 4f). Indeed, away from the influence of hydrothermal vents (104), low deep ocean Mn concentrations (68, 114) as a consequence of strong oxidative scavenging (94) result in Mn being estimated to be the most deficient nutrient throughout the Atlantic at depths >600m (Figure 7c).

Dissolved Mn is frequently elevated in the surface waters of the low latitudes as a result of atmospheric inputs alongside increased solubility due to photoreduction (114-116). However, concentrations in the surface SO can be very low and are associated with marked near surface depletion (68, 100, 116) alongside some evidence suggesting the potential for (co-)limitation by this element alongside Fe (110, 112, 113). In the context of the large scale oceanic circulation, strong upwelling of Mn deficient deep waters (>600m) within the SO (Figure 4f & 7 c, d) may thus contribute to the potential for development of any such Mn (co-)limitation.

The micronutrient Zn has a wide range of metabolic roles (28). Although substitutions might maintain some metabolic activities under reduced Zn availability (12, 19, 54), there is limited experimental evidence for Zn (co-)limitation of at least some phytoplankton groups in certain regions (111, 117-119). Performing a calculation of the relative deficiency between Zn, Fe, N and P for the Atlantic Ocean IDP2014 data (Figure 7 e, f) also reveals an interesting pattern. Primary Zn deficiency is not typically estimated within surface waters. However, near sub-surface thermocline waters down to a maximum of ~600m within the (sub-)tropics (around 50°N to 50°S), alongside the nearer surface waters of at the northern and southern boundaries of this region, display a tendency for Zn to be either most or second most deficient of the 4 considered nutrients (Figure 7 e,f). The distinction between 1° or 2° being sensitive to the assumed Fe:N ratio in this case (Figure 7 e,f). The relative deficiency of Zn within the thermocline of the Atlantic presumably reflects the low Zn concentrations within the Sub-Antarctic Mode Waters (SAMW) which act as a major source of water to the global thermocline and hence low latitude surface waters (39, 43). The associated relative depletion of Zn within these near surface waters thus has the potential to play a role in surface biogeochemistry, for example through influencing the ability of organisms to utilise Zn forms of alkaline phosphatase in accessing dissolved organic P (119, 120).

Uncertainties associated with stoichiometric plasticity: returning to the system context

Sensitivity analyses (Figure 7) and the proceeding largely qualitative descriptions of derived patterns and their subsequent implications for ocean biogeochemistry, suggest that reasonably insightful inference can be gained from calculations of nutrient deficiency using the unprecedented oceanic scale high quality multi-element data within the GEOTRACES IDP2014 (21). However, remaining considerable unknowns concerning the variability in, and controls on, cellular stoichiometric plasticity remain problematic. Consideration of deficiencies with respect to the macronutrient N, which displays by far the least stoichiometric plasticity (with reference to C) for the potentially limiting nutrients (11), partially simplifies this complex problem. However marked stoichiometric plasticity characterises intracellular quotas for many of the trace metals, both within and between groups (44) and likely occurs alongside variability in the stoichiometric processing of elements during biogeochemical transformations (12, 29).

Uptake ratios within newly formed organic matter are of central importance within the context of deficiency. Moreover, within complex mixed microbial communities, the stoichiometry of those organisms dominating the overall production of new biomass will both set the availability of nutrients for other components of the community (55) and, by definition, will have a dominant role in driving overall biological requirements for the different nutrients. Despite the high stoichiometric plasticity which can be observed in mono-culture experiments, there is evidence that stoichiometric ratios within natural communities may be more constrained (44). It is thus valid to ask whether the extremes of plasticity observable in mono-cultures, including high quotas under conditions of high excess trace metal (bio-)availability and in particular the low quotas associated with severe nutrient limitation, might be expected to be fully expressed at the level of mixed communities within the natural system (121). Net growth rates of organisms within natural communities will be a function of both bottom up and top down controls (122) such that microbes under severe growth rate nutrient limitation are likely to be rapidly outcompeted (121). Thus, it might be hypothesised that the majority of new biomass would actually be produced by cells which are not severely nutrient limited and which hence have nutrient quotas towards the higher end of observed ranges (Figure 1). However, markedly low Fe quotas within certain SO taxa (123) suggest that considerable taxonomic adaptation to reduced Fe occurs.

Wider application of tools capable of assessing the extent of stoiciohometric plasticity within natural communities is thus clearly desirable (44). Particularly as a lot of potential information is currently lost through using the non-quantitative approach adopted above. For example, it is highly likely that NADW is actually significantly less deficient in Fe than AABW (37), however the quantitative implications of this for ocean biogeochemistry remain difficult to assess. Thus, in the current initial analysis, the conservative choice of a marker of deficiency which is less sensitive to current poorly understood variability in $R_{X:Y}$ has necessarily been traded off against the added quantitative information which could be derived were a more complete understanding of variability in such ratios available across large scales within natural microbial communities.

Summary and conclusions

Analysis of the data contained within the GEOTRACES IDP2014 confirms that the open ocean, or at least the Atlantic, is stoichiometricaly deficient in Fe everywhere outside of the macro-nutrient (N,P) depleted surface (sub-)tropical waters. Such a conclusion appears to be reasonably robust to caveats associated with the plasticity of phytoplankton Fe:N ratios. Sub-surface waters below 600m appear to be further deficient in Mn. However, the extent of subsurface oceanic Mn deficiency relative to Fe is reasonably sensitive to assumptions concerning Mn:Fe ratios. Thermocline waters of the Atlantic also appear to be relatively deficient in Zn, although the uncertainties in such conclusions begin to become considerable when 3 or more trace metals and flexibility in their relative biological ratios is considered.

Trace metal deficiencies within the sub-surface ocean are consistent with the predominance of Fe limitation within strong upwelling systems, including the globally dominant SO, being largely a result of the upwelling (97, 100). Deep ocean trace metal sources may thus be important in the context of large scale oceanic transports (104). However, it is reiterated that sub-surface nutrient deficiency is only one of the factors which needs to be considered in any complete understanding of upper ocean nutrient limitation, with external supplies to surface waters from sediments (34, 35) and the atmosphere (33), alongside non-stoichometric ecosystem processes, likely to be important in many cases (11).

More generally, ranking of relative deficiencies amongst potentially (co-)limiting trace metals is reasonably sensitive to decisions concerning which are included in any given calculation and assumptions concerning the assumed biological ratios. Such analysis serves to further highlight how an enhanced understanding of the controls on variable intracellular trace metal stoichiometry will be crucial in developing a more complete understanding of trace element cycling. Similar to consideration of an idealised N, P, Fe, non-diazotroph, diazotroph system (Figure 6), fuller understanding of the multi-nutrient ocean requires appreciation of availability versus the relative requirements of different nutrients within biological systems (28, 29), alongside theoretical frameworks (19, 24, 26) capable of capturing nutrient-biota feedback cycles and the variable stoichiometry of the organisms which drive them.

Additional Information

Information on the following should be included wherever relevant.

Data accessibility
All of the data analysed within the current contribution is publically available within the GEOTRACES Intermediate Data Product 2014 (Mawji, E., et al., The GEOTRACES Intermediate Data Product 2014, Mar. Chem. (2015), http://dx.doi.org/10.1016/j.marchem.2015.04.005)

Acknowledgments
This work would not have been possible without the generation and release of the high quality multi-element data within the GEOTRACES Intermediate Data Product 2014. I therefore wish to acknowledge and thank all of the scientists involved in the establishment and running of the International GEOTRACES project and particularly those who made their data publically available within the IDP2014, alongside the funding agencies which supported their work. The author's research was directly supported by the Natural Environment Research Council (NERC) UK through grants NE/H004394/1 and NE/K015613/1.

Competing Interests
I have no competing interests.

References

1. Redfield A. C. 1958 The biological control of chemical factors in the environment. *American Scientist*. **46** 205-91.
2. Whitfield M. 2001 Interactions between phytoplankton and trace metals in the ocean. *Adv Mar Biol*. **41** 1-128.
3. Broecker W. S., Peng T. H. 1982 Tracers in the Sea. *Lamont-Doherty Geological Observatory, Columbia University*.
4. Volk T., Hoffert M. I. 1985 Ocean carbon pumps - Analysis of relative strengths and efficiencies in ocean-driven atmospheric CO2 changes. *in: The Carbon Cycle and Atmospheric CO2: Natural VariationsArchaean to Present, Geophys Monogr Ser, vol 32, edited by E T Sundquist and W S Broecker, 99–110, AGU, Washington, D C*.
5. Sarmiento J. L., Toggweiler J. R. 1984 A new model for the role of the ocean in determining atmospheric pCO2. *Nature*. **308** 621-4.
6. Siegenthaler U., Wenk T. 1984 Rapid atmospheric CO2 variations and ocean circulation. *Nature*. **308** 624-6.
7. Sigman D. M., Hain M. P., Haug G. H. 2010 The polar ocean and glacial cycles in atmospheric CO2 concentration. *Nature*. **466** 47-55.
8. Blackman F. F. 1905 Optima and limiting factors. *Ann Bot*. **19** 281-9.
9. von Liebig J. 1840 Chemistry and its Application to Agriculture And Physiology. *(Taylor and Walton, London*.
10. Arrigo K. R. 2005 Marine microorganisms and global nutrient cycles. *Nature*. **437** 349-55.
11. Moore C. M., Mills M. M., Arrigo K. R., Berman-Frank I., Bopp L., Boyd P. W., Galbraith E. D., Geider R. J., Guieu C., Jaccard S. L., et al. 2013 Processes and patterns of oceanic nutrient limitation. *Nat Geosci*. **6** 701-10.
12. Sunda W. G. 2012 Feedback interactions between trace metal nutrients and phytoplankton in the ocean. *Front Microbiol*. **3** 22.

13. Falkowski P., Scholes R. J., Boyle E., Canadell J., Canfield D., Elser J., Gruber N., Hibbard K., Hogberg P., Linder S., et al. 2000 The global carbon cycle: A test of our knowledge of earth as a system. *Science*. **290** 291-6.

14. Saito M. A., Sigman D. M., Morel F. M. M. 2003 The bioinorganic chemistry of the ancient ocean: the co-evolution of cyanobacterial metal requirements and biogeochemical cycles at the Archean-Proterozoic boundary? *Inorg Chim Acta*. **356** 308-18.

15. Martinez-Garcia A., Sigman D. M., Ren H. J., Anderson R. F., Straub M., Hodell D. A., Jaccard S. L., Eglinton T. I., Haug G. H. 2014 Iron Fertilization of the Subantarctic Ocean During the Last Ice Age. *Science*. **343** 1347-50.

16. Whitfield M. 2001 Interactions between phytoplankton and trace metals in the ocean. *Advances in Marine Biology*. **41** 1-128.

17. Debaar H. J. W. 1994 von Liebig law of the minimum and plankton ecology (1899-1991). *Progress in Oceanography*. **33** 347-86.

18. Martin J. H., Fitzwater S. E. 1988 Iron-deficiency limits phytoplankton growth in the Northeast Pacific SubArctic. *Nature*. **331** 341-3.

19. Saito M. A., Goepfert T. J., Ritt J. T. 2008 Some thoughts on the concept of colimitation: Three definitions and the importance of bioavailability. *Limnology and Oceanography*. **53** 276-90.

20. Boyd P. W., Jickells T., Law C. S., Blain S., Boyle E. A., Buesseler K. O., Coale K. H., Cullen J. J., de Baar H. J. W., Follows M., et al. 2007 Mesoscale iron enrichment experiments 1993-2005: Synthesis and future directions. *Science*. **315** 612-7.

21. Mawji E., Schlitzer R., Dodas E. M., Abadie C., Abouchami W., Anderson R. F., Baars O., Bakker K., Baskaran M., Bates N. R., et al. 2015 The GEOTRACES Intermediate Data Product 2014. *Marine Chemistry*. **177** 1-8.

22. Cullen J. J. 1991 Hypotheses to explain high-nutrient conditions in the open sea. *Limnology and Oceanography*. **36** 1578-99.

23. Tilman D., Kilham S. S., Kilham P. 1982 Phytoplankton community ecology - The role of limiting nutrients. *Annu Rev Ecol Syst*. **13** 349-72.

24. Tilman D. 1980 Resources - A graphical-mechanistic approach to competition and predation. *Am Nat*. **116** 362-93.

25. Snow J. T., Schlosser C., Woodward E. M. S., Mills M. M., Achterberg E. P., Mahaffey C., Bibby T. S., Moore C. M. 2015 Environmental controls on the biogeography of diazotrophy and Trichodesmium in the Atlantic Ocean. *Global Biogeochemical Cycles*. **29** 865-84.

26. Ward B. A., Dutkiewicz S., Moore C. M., Follows M. J. 2013 Iron, phosphorus, and nitrogen supply ratios define the biogeography of nitrogen fixation. *Limnology and Oceanography*. **58** 2059-75.

27. Dutkiewicz S., Follows M. J., Bragg J. G. 2009 Modeling the coupling of ocean ecology and biogeochemistry. *Global Biogeochemical Cycles*. **23** 15.

28. Frausto da Silva J. J. R., Williams R. J. P. 2001 The Biological Chemistry of the Elements: The Inorganic Chemistry of Life, 2nd edn *(Oxford Univ Press)*

29. Sterner R. W., Elser J. J. 2002 Ecological Stoichiometry: The Biology of Elements from Molecules to the Biosphere *Princeton Univ Press*.

30. Redfield A.C. 1934 On the proportions of organic derivations in sea water and their relation to the composition of plankton. *In James Johnstone Memorial Volume (ed RJ Daniel) University Press of Liverpool, pp 176–192*.

31. Deutsch C., Sarmiento J. L., Sigman D. M., Gruber N., Dunne J. P. 2007 Spatial coupling of nitrogen inputs and losses in the ocean. *Nature*. **445** 163-7.

32. Klausmeier C. A., Litchman E., Levin S. A. 2004 Phytoplankton growth and stoichiometry under multiple nutrient limitation. *Limnology and Oceanography*. **49** 1463-70.

33. Jickells T. D., An Z. S., Andersen K. K., Baker A. R., Bergametti G., Brooks N., Cao J. J., Boyd P. W., Duce R. A., Hunter K. A., et al. 2005 Global iron connections between desert dust, ocean biogeochemistry, and climate. *Science*. **308** 67-71.

34. Homoky W. B., John S. G., Conway T. M., Mills R. A. 2013 Distinct iron isotopic signatures and supply from marine sediment dissolution. *Nat Commun*. **4** 10.

35. Severmann S., McManus J., Berelson W. M., Hammond D. E. 2010 The continental shelf benthic iron flux and its isotope composition. *Geochimica Et Cosmochimica Acta*. **74** 3984-4004.

36. Lam P. J., Bishop J. K. B. 2008 The continental margin is a key source of iron to the HNLC North Pacific Ocean. *Geophysical Research Letters*. **35**.

37. Parekh P., Follows M. J., Boyle E. A. 2005 Decoupling of iron and phosphate in the global ocean. *Global Biogeochemical Cycles*. **19**.

38. Gruber N., Sarmiento J. L. 1997 Global patterns of marine nitrogen fixation and denitrification. *Global Biogeochemical Cycles*. **11** 235-66.

39. Sarmiento J. L., Gruber N., Brzezinski M. A., Dunne J. P. 2004 High-latitude controls of thermocline nutrients and low latitude biological productivity. *Nature*. **427** 56-60.

40. Deutsch C., Gruber N., Key R. M., Sarmiento J. L., Ganachaud A. 2001 Denitrification and N-2 fixation in the Pacific Ocean. *Global Biogeochemical Cycles*. **15** 483-506.

41. Deutsch C., Weber T. 2012 Nutrient Ratios as a Tracer and Driver of Ocean Biogeochemistry. *Annual Review of Marine Science*. **4** 113-41.

42. Janssen D. J., Conway T. M., John S. G., Christian J. R., Kramer D. I., Pedersen T. F., Cullen J. T. 2014 Undocumented water column sink for cadmium in open ocean oxygen-deficient zones. *Proceedings of the National Academy of Sciences of the United States of America*. **111** 6888-93.

43. Wyatt N. J., Milne A., Woodward E. M. S., Rees A. P., Browning T. J., Bouman H. A., Worsfold P. J., Lohan M. C. 2014 Biogeochemical cycling of dissolved zinc along the GEOTRACES South Atlantic transect GA10 at 40 S. *Global Biogeochemical Cycles*. **28** 44-56.

44. Twining B. S., Baines S. B. 2013 The Trace Metal Composition of Marine Phytoplankton. *Annual Review of Marine Science*. **5** 191-215.

45. Martiny A. C., Pham C. T. A., Primeau F. W., Vrugt J. A., Moore J. K., Levin S. A., Lomas M. W. 2013 Strong latitudinal patterns in the elemental ratios of marine plankton and organic matter. *Nat Geosci*. **6** 279-83.

46. DeVries T., Deutsch C. 2014 Large-scale variations in the stoichiometry of marine organic matter respiration. *Nat Geosci*. **7** 890-4.

47. Teng Y. C., Primeau F. W., Moore J. K., Lomas M. W., Martiny A. C. 2014 Global-scale variations of the ratios of carbon to phosphorus in exported marine organic matter. *Nat Geosci*. **7** 895-8.

48. Lane E. S., Semeniuk D. M., Strzepek R. F., Cullen J. T., Maldonado M. T. 2009 Effects of iron limitation on intracellular cadmium of cultured phytoplankton: Implications for surface dissolved cadmium to phosphate ratios. *Marine Chemistry*. **115** 155-62.

49. Sunda W. G., Huntsman S. A. 2000 Effect of Zn, Mn, and Fe on Cd accumulation in phytoplankton: Implications for oceanic Cd cycling. *Limnology and Oceanography*. **45** 1501-16.

50. Sunda W. G., Huntsman S. A. 1996 Antagonisms between cadmium and zinc toxicity and manganese limitation in a coastal diatom. *Limnology and Oceanography*. **41** 373-87.

51. Horner T. J., Lee R. B. Y., Henderson G. M., Rickaby R. E. M. 2013 Nonspecific uptake and homeostasis drive the oceanic cadmium cycle. *Proceedings of the National Academy of Sciences of the United States of America*. **110** 2500-5.

52. Sunda W. G., Huntsman S. A. 1995 Iron uptake and growth limitation in oceanic and coastal phytoplankton. *Marine Chemistry*. **50** 189-206.

53. Marchetti A., Parker M. S., Moccia L. P., Lin E. O., Arrieta A. L., Ribalet F., Murphy M. E. P., Maldonado M. T., Armbrust E. V. 2009 Ferritin is used for iron storage in bloom-forming marine pennate diatoms. *Nature*. **457** 467-70.

54. Sunda W. G., Huntsman S. A. 1995 Cobalt and zinc interreplacement in marine phytoplankton: Biological and geochemical implications. *Limnology and Oceanography*. **40** 1404-17.

55. Mills M. M., Arrigo K. R. 2010 Magnitude of oceanic nitrogen fixation influenced by the nutrient uptake ratio of phytoplankton. *Nat Geosci*. **3** 412-6.

56. Weber T. S., Deutsch C. 2010 Ocean nutrient ratios governed by plankton biogeography. *Nature*. **467** 550-4.

57. Weber T., Deutsch C. 2012 Oceanic nitrogen reservoir regulated by plankton diversity and ocean circulation. *Nature*. **489** 419-U105.

58. Anderson R. F., Mawji E., Cutter G. A., Measures C. I., Jeandel C. 2014 GEOTRACES Changing the Way We Explore Ocean Chemistry. *Oceanography*. **27** 50-61.

59. Henderson G. M., Anderson R. F., Adkins J., Andersson P., Boyle E. A., Cutter G., de Baar H., Eisenhauer A., Frank M., Francois R., et al. 2007 GEOTRACES - An international study of the global marine biogeochemical cycles of trace elements and their isotopes. *Chemie Der Erde-Geochemistry*. **67** 85-131.

60. Cutter G. A. 2013 Intercalibration in chemical oceanography-Getting the right number. *Limnology and Oceanography-Methods*. **11** 418-24.

61. Bowie A. R., Griffiths F. B., Dehairs F., Trull T. W. 2011 Oceanography of the subantarctic and Polar Frontal Zones south of Australia during summer: Setting for the SAZ-Sense study. *Deep-Sea Research Part Ii-Topical Studies in Oceanography*. **58** 2059-70.

62. van Heuven S., Hoppema M., Huhn O., Slagter H. A., de Baar H. J. W. 2011 Direct observation of increasing CO2 in the Weddell Gyre along the Prime Meridian during 1973-2008. *Deep-Sea Research Part Ii-Topical Studies in Oceanography*. **58** 2613-35.

63. Rijkenberg M. J. A., Middag R., Laan P., Gerringa L. J. A., van Aken H. M., Schoemann V., de Jong J. T. M., de Baar H. J. W. 2014 The Distribution of Dissolved Iron in the West Atlantic Ocean. *Plos One*. **9**.

64. Ericson Y., Ulfsbo A., van Heuven S., Kattner G., Anderson L. G. 2014 Increasing carbon inventory of the intermediate layers of the Arctic Ocean. *Journal of Geophysical Research-Oceans*. **119** 2312-26.

65. Salt L. A., van Heuven S., Claus M. E., Jones E. M., de Baar H. J. W. 2015 Rapid acidification of mode and intermediate waters in the southwestern Atlantic Ocean. *Biogeosciences*. **12** 1387-401.

66. Middag R., van Hulten M. M. P., Van Aken H. M., Rijkenberg M. J. A., Gerringa L. J. A., Laan P., de Baar H. J. W. 2015 Dissolved aluminium in the ocean conveyor of the West Atlantic Ocean: Effects of the biological cycle, scavenging, sediment resuspension and hydrography. *Marine Chemistry*. **177** 69-86.

67. Chever F., Bucciarelli E., Sarthou G., Speich S., Arhan M., Penven P., Tagliabue A. 2010 Physical speciation of iron in the Atlantic sector of the Southern Ocean along a transect from the subtropical domain to the Weddell Sea Gyre. *Journal of Geophysical Research-Oceans*. **115** 15.

68. Middag R., de Baar H. J. W., Laan P., Cai P. H., van Ooijen J. C. 2011 Dissolved manganese in the Atlantic sector of the Southern Ocean. *Deep-Sea Research Part Ii-Topical Studies in Oceanography*. **58** 2661-77.

69. Croot P. L., Baars O., Streu P. 2011 The distribution of dissolved zinc in the Atlantic sector of the Southern Ocean. *Deep-Sea Research Part Ii-Topical Studies in Oceanography*. **58** 2707-19.

70. Middag R., de Baar H. J. W., Laan P., Huhn O. 2012 The effects of continental margins and water mass circulation on the distribution of dissolved aluminum and manganese in Drake Passage. *Journal of Geophysical Research-Oceans*. **117**.

71. Klunder M. B., Laan P., Middag R., De Baar H. J. W., van Ooijen J. C. 2011 Dissolved iron in the Southern Ocean (Atlantic sector). *Deep-Sea Research Part Ii-Topical Studies in Oceanography*. **58** 2678-94.

72. Abouchami W., Galer S. J. G., de Baar H. J. W., Middag R., Vance D., Zhao Y., Klunder M., Mezger K., Feldmann H., Andreae M. O. 2014 Biogeochemical cycling of cadmium isotopes in the Southern Ocean along the Zero Meridian. *Geochimica Et Cosmochimica Acta*. **127** 348-67.

73. Boye M., Wake B. D., Garcia P. L., Bown J., Baker A. R., Achterberg E. P. 2012 Distributions of dissolved trace metals (Cd, Cu, Mn, Pb, Ag) in the southeastern Atlantic and the Southern Ocean. *Biogeosciences*. **9** 3231-46.

74. Klunder M. B., Laan P., Middag R., de Baar H. J. W., Bakker K. 2012 Dissolved iron in the Arctic Ocean: Important role of hydrothermal sources, shelf input and scavenging removal. *Journal of Geophysical Research-Oceans*. **117**.

75. Vu H. T. D., Sohrin Y. 2013 Diverse stoichiometry of dissolved trace metals in the Indian Ocean. *Sci Rep*. **3** 5.

76. Saito M. A., Noble A. E., Tagliabue A., Goepfert T. J., Lamborg C. H., Jenkins W. J. 2013 Slow-spreading submarine ridges in the South Atlantic as a significant oceanic iron source. *Nat Geosci*. **6** 775-9.

77. Baars O., Abouchami W., Galer S. J. G., Boye M., Croot P. L. 2014 Dissolved cadmium in the Southern Ocean: Distribution, speciation, and relation to phosphate. *Limnology and Oceanography*. **59** 385-99.

78. Hatta M., Measures C. I., Wu J. F., Roshan S., Fitzsimmons J. N., Sedwick P., Morton P. 2015 An overview of dissolved Fe and Mn distributions during the 2010-2011 US GEOTRACES north Atlantic cruises: GEOTRACES GA03. *Deep-Sea Research Part Ii-Topical Studies in Oceanography*. **116** 117-29.

79. Conway T. M., John S. G. 2014 The biogeochemical cycling of zinc and zinc isotopes in the North Atlantic Ocean. *Global Biogeochemical Cycles*. **28** 1111-28.

80. Lannuzel D., Bowie A. R., Remenyi T., Lam P., Townsend A., Ibisanmi E., Butler E., Wagener T., Schoemann V. 2011 Distributions of dissolved and particulate iron in the sub-Antarctic and Polar Frontal Southern Ocean (Australian sector). *Deep-Sea Research Part Ii-Topical Studies in Oceanography*. **58** 2094-112.

81. Roshan S., Wu J. F. 2015 Water mass mixing: The dominant control on the zinc distribution in the North Atlantic Ocean. *Global Biogeochemical Cycles*. **29** 1060-74.

82. Butler E. C. V., O'Sullivan J. E., Watson R. J., Bowie A. R., Remenyi T. A., Lannuzel D. 2013 Trace metals Cd, Co, Cu, Ni, and Zn in waters of the subantarctic and Polar Frontal Zones south of Tasmania during the 'SAZ-Sense' project. *Marine Chemistry*. **148** 63-76.

83. Noble A. E., Lamborg C. H., Ohnemus D. C., Lam P. J., Goepfert T. J., Measures C. I., Frame C. H., Casciotti K. L., DiTullio G. R., Jennings J., et al. 2012 Basin-scale inputs of cobalt, iron, and manganese from the Benguela-Angola front to the South Atlantic Ocean. *Limnology and Oceanography*. **57** 989-1010.

84. Middag R., van Slooten C., de Baar H. J. W., Laan P. 2011 Dissolved aluminium in the Southern Ocean. *Deep-Sea Research Part Ii-Topical Studies in Oceanography*. **58** 2647-60.

85. Measures C., Hatta M., Fitzsimmons J., Morton P. 2015 Dissolved Al in the zonal N Atlantic section of the US GEOTRACES 2010/2011 cruises and the importance of hydrothermal inputs. *Deep-Sea Research Part Ii-Topical Studies in Oceanography*. **116** 176-86.

86. Ho T. Y., Quigg A., Finkel Z. V., Milligan A. J., Wyman K., Falkowski P. G., Morel F. M. M. 2003 The elemental composition of some marine phytoplankton. *Journal of Phycology*. **39** 1145-59.

87. Schlosser C., Klar J. K., Wake B. D., Snow J. T., Honey D. J., Woodward E. M. S., Lohan M. C., Achterberg E. P., Moore C. M. 2014 Seasonal ITCZ migration dynamically controls the location of the (sub)tropical Atlantic biogeochemical divide. *Proceedings of the National Academy of Sciences of the United States of America*. **111** 1438-42.

88. Raven J. A. 1988 The iron and molybdenum use efficiencies of plant-growth with differen energy, carbon and nitrogen-sources. *New Phytologist*. **109** 279-87.

89. Kustka A., Sanudo-Wilhelmy S., Carpenter E. J., Capone D. G., Raven J. A. 2003 A revised estimate of the iron use efficiency of nitrogen fixation, with special reference to the marine cyanobacterium Trichodesmium spp. (Cyanophyta). *Journal of Phycology*. **39** 12-25.

90. Gledhill M., Buck K. N. 2012 The organic complexation of iron in the marine environment: a review. *Front Microbiol*. **3**.

91. Boyd P. W., Ellwood M. J. 2010 The biogeochemical cycle of iron in the ocean. *Nat Geosci*. **3** 675-82.

92. Wu J. F., Sunda W., Boyle E. A., Karl D. M. 2000 Phosphate depletion in the western North Atlantic Ocean. *Science*. **289** 759-62.

93. Moore C. M., Mills M. M., Achterberg E. P., Geider R. J., LaRoche J., Lucas M. I., McDonagh E. L., Pan X., Poulton A. J., Rijkenberg M. J. A., et al. 2009 Large-scale distribution of Atlantic nitrogen fixation controlled by iron availability. *Nat Geosci*. **2** 867-71.

94. Li Y. H. 1991 Distribution patterns of the elements in the ocean - a synthesis. *Geochimica Et Cosmochimica Acta*. **55** 3223-40.

95. Johnson K. S., Gordon R. M., Coale K. H. 1997 What controls dissolved iron concentrations in the world ocean? *Marine Chemistry*. **57** 137-61.

96. Behrenfeld M. J., Worthington K., Sherrell R. M., Chavez F. P., Strutton P., McPhaden M., Shea D. M. 2006 Controls on tropical Pacific Ocean productivity revealed through nutrient stress diagnostics. *Nature*. **442** 1025-8.

97. Coale K. H., Fitzwater S. E., Gordon R. M., Johnson K. S., Barber R. T. 1996 Control of community growth and export production by upwelled iron in the equatorial Pacific Ocean. *Nature*. **379** 621-4.

98. Ryan-Keogh T. J., Macey A. I., Nielsdottir M. C., Lucas M. I., Steigenberger S. S., Stinchcombe M. C., Achterberg E. P., Bibby T. S., Moore C. M. 2013 Spatial and temporal development of phytoplankton iron stress in relation to bloom dynamics in the high-latitude North Atlantic Ocean. *Limnology and Oceanography*. **58** 533-45.

99. Marshall J., Speer K. 2012 Closure of the meridional overturning circulation through Southern Ocean upwelling. *Nat Geosci*. **5** 171-80.

100. Martin J. H., Gordon R. M., Fitzwater S. E. 1990 Iron in Antarctic waters. *Nature*. **345** 156-8.

101. Tagliabue A., Sallee J. B., Bowie A. R., Levy M., Swart S., Boyd P. W. 2014 Surface-water iron supplies in the Southern Ocean sustained by deep winter mixing. *Nat Geosci*. **7** 314-20.

102. Tagliabue A., Bopp L., Dutay J.-C., Bowie A. R., Chever F., Jean-Baptiste P., Bucciarelli E., Lannuzel D., Remenyi T., Sarthou G., et al. 2010 Hydrothermal contribution to the oceanic dissolved iron inventory. *Nat Geosci*. **3** 252-6.

103. Fitzsimmons J. N., Boyle E. A., Jenkins W. J. 2014 Distal transport of dissolved hydrothermal iron in the deep South Pacific Ocean. *Proceedings of the National Academy of Sciences of the United States of America*. **111** 16654-61.

104. Resing J. A., Sedwick P. N., German C. R., Jenkins W. J., Moffett J. W., Sohst B. M., Tagliabue A. 2015 Basin-scale transport of hydrothermal dissolved metals across the South Pacific Ocean. *Nature*. **523** 200-3.

105. Bennett S. A., Achterberg E. P., Connelly D. P., Statham P. J., Fones G. R., German C. R. 2008 The distribution and stabilisation of dissolved Fe in deep-sea hydrothermal plumes. *Earth and Planetary Science Letters*. **270** 157-67.

106. Horner T. J., Williams H. M., Hein J. R., Saito M. A., Burton K. W., Halliday A. N., Nielsen S. G. 2015 Persistence of deeply sourced iron in the Pacific Ocean. *Proceedings of the National Academy of Sciences of the United States of America*. **112** 1292-7.

107. Sohm J. A., Webb E. A., Capone D. G. 2011 Emerging patterns of marine nitrogen fixation. *Nature Reviews Microbiology*. **9** 499-508.

108. Sanudo-Wilhelmy S. A., Kustka A. B., Gobler C. J., Hutchins D. A., Yang M., Lwiza K., Burns J., Capone D. G., Raven J. A., Carpenter E. J. 2001 Phosphorus limitation of nitrogen fixation by Trichodesmium in the central Atlantic Ocean. *Nature*. **411** 66-9.

109. Conway T. M., John S. G. 2014 Quantification of dissolved iron sources to the North Atlantic Ocean. *Nature*. **511** 212-5.

110. Buma A. G. J., Debaar H. J. W., Nolting R. F., Vanbennekom A. J. 1991 Metal enrichment experiments in the Weddel-Scotia seas - Effects of iron and manganese on various plankton communities. *Limnology and Oceanography*. **36** 1865-78.

111. Coale K. H. 1991 Effects of iron, manganese, copper and zinc enrichments on productivity and biomass in the Sub-Arctic Pacific. *Limnology and Oceanography*. **36** 1851-64.

112. Middag R., de Baar H. J. W., Klunder M. B., Laan P. 2013 Fluxes of dissolved aluminum and manganese to the Weddell Sea and indications for manganese co-limitation. *Limnology and Oceanography*. **58** 287-300.

113. Browning T. J., Bouman H. A., Henderson G. M., Mather T. A., Pyle D. M., Schlosser C., Woodward E. M. S., Moore C. M. 2014 Strong responses of Southern Ocean phytoplankton communities to volcanic ash. *Geophysical Research Letters*. **41** 2851-7.

114. Landing W. M., Bruland K. W. 1980 Manganese in the North Pacific. *Earth and Planetary Science Letters*. **49** 45-56.

115. Sunda W. G., Huntsman S. A., Harvey G. R. 1983 Photo-reduction of manganese oxides in seawater and its geochemical and biological implications. *Nature*. **301** 234-6.

116. Shiller A. M. 1997 Manganese in surface waters of the Atlantic Ocean. *Geophysical Research Letters*. **24** 1495-8.

117. Lohan M. C., Crawford D. W., Purdie D. A., Statham P. J. 2005 Iron and zinc enrichments in the northeastern subarctic Pacific: Ligand production and zinc availability in response to phytoplankton growth. *Limnology and Oceanography*. **50** 1427-37.

118. Crawford D. W., Lipsen M. S., Purdie D. A., Lohan M. C., Statham P. J., Whitney F. A., Putland J. N., Johnson W. K., Sutherland N., Peterson T. D., et al. 2003 Influence of zinc and iron enrichments on phytoplankton growth in the northeastern subarctic Pacific. *Limnology and Oceanography*. **48** 1583-600.
119. Jakuba R. W., Moffett J. W., Dyhrman S. T. 2008 Evidence for the linked biogeochemical cycling of zinc, cobalt, and phosphorus in the western North Atlantic Ocean. *Global Biogeochemical Cycles*. **22** 13.
120. Shaked Y., Xu Y., Leblanc K., Morel F. M. M. 2006 Zinc availability and alkaline phosphatase activity in Emiliania huxleyi: Implications for Zn-P co-limitation in the ocean. *Limnology and Oceanography*. **51** 299-309.
121. Boyd P. W., Strzepek R. F., Ellwood M. J., Hutchins D. A., Nodder S. D., Twining B. S., Wilhelm S. W. 2015 Why are biotic iron pools uniform across high- and low-iron pelagic ecosystems? *Global Biogeochemical Cycles*. **29** 1028-43.
122. Banse K. 2013 Reflections About Chance in My Career, and on the Top-Down Regulated World. *Annual Review of Marine Science*. **5** 1-19.
123. Strzepek R. F., Maldonado M. T., Hunter K. A., Frew R. D., Boyd P. W. 2011 Adaptive strategies by Southern Ocean phytoplankton to lessen iron limitation: Uptake of organically complexed iron and reduced cellular iron requirements. *Limnology and Oceanography*. **56** 1983-2002.

Figure and table captions

Figure 1 Plot of the stoichiometry of different nutrient elements in phytoplankton cellular material against the dissolved concentration stoichiometry within Antarctic Circumpolar Deep Water (CDW). Open symbols are plotted at a point on the abscissa corresponding to the mean values across a range of different phytoplankton taxa as previously adopted (11, 86), with the horizontal bars representing the maximum range of stoichiometric variability which has currently been observed in culture for these elements (see (11) for further discussion), updated where applicable (123). Open symbols are plotted at a point on the ordinate corresponding to the mean concentration of that element observed within CDW (potential temperature from 1-2°C, salinity from 34.62-34.73), from the GEOTRACES intermediate data product (21), with vertical bars (where visible) representing 1 standard deviation of the average concentration. The solid diagonal line delineates nutrients which are more replete or deficient with respect to N within this water mass.

Figure 2 Plot of ‘typical’ phytoplankton cellular stoichiometry against measured dissolved stoichiometry (see Figure 1) from the thermocline of the North Atlantic sub-tropical gyre (>25°N - <35°N) from the GEOTRACES intermediate data product (21). For clarity/simplicity, known stoichiometric flexibility is disregarded. Nutrients which have equal availability relative to biological demands would lie along parallels as indicated by the diagonal solid lines, with individual lines separated by 1 order of magnitude. Insets to right show subsections of main plot with relative deficits/excesses between nutrient pairs expressed as linear combinations using the typical ‘*’ notation schematically illustrated by the thick coloured lines.

Figure 3 Comparison of a previous compilation of experimental evidence (11) of upper ocean primary nutrient limitation (a) and calculation upper ocean primary nutrient deficiency based on the IDP2014 (b).

Figure 4 Plots of biological nutrient quotas against dissolved nutrient ratios as derived from the GEOTRACES IDP2014 for a range of water masses: a) surface waters of the North Atlantic Sub-tropical Gyre (NASG), b) surface waters of the high latitude North Atlantic sub-polar Gyre (NASPG), c) surface waters of the Southern Ocean (SO), d) thermocline waters of the NASG, e) North Atlantic Deep Water (NADW), f) Southern Ocean Circumpolar Deep Water (CDW). Solid symbols are plotted at the assumed typical biological ratio, with the thick horizontal lines for Fe and Mn indicating an order of magnitude lower estimate (see text).

Figure 5 Relative deficiency between the nutrients N, P and Fe for a full depth section through the Atlantic Ocean derived from data within the GEOTRACES IDP2014. Colour scheme as in Figure 3. Schematic large scale ocean circulation patterns are indicated, alongside indicative positions of water masses discussed in the text.

Figure 6 Primary (a, b) and Secondary (c, d) deficiency varying between N, P and Fe across different oceanic nutrient provinces as a function of (a, c) imposed changes in external Fe supply relative to stoichiometric requirements (here for simplicity just rescaled (0-1) between no external supply and a highly enriched supply) within a simple idealised model, compared to (b, d) observations of relative N, P and Fe deficiency in surface waters across an inferred broad scale gradient in atmospheric dust inputs on the basis of dissolved Al data within the IDP2014 from the Atlantic Ocean.

Figure 7 Estimated primary (a, c, e) and secondary (b, d, f) deficiency between subsets of nutrients for a full depth section through the Atlantic Ocean derived from data within the GEOTRACES IDP2014. Deficiency is estimated using the assumed typical biological stoichiometry (small symbols) and a stoichiometry involving an assumed order of magnitude lower quota for both the Fe and Mn (large symbols). Calculations are performed considering just N (blue), P (black) and Fe (red) (a, b), N (blue), P (black), Fe (red) and Mn (green) (c, d) and N (blue), P (black), Fe (red) and Zn (yellow) (e, f). Note the logarithmic depth axis.

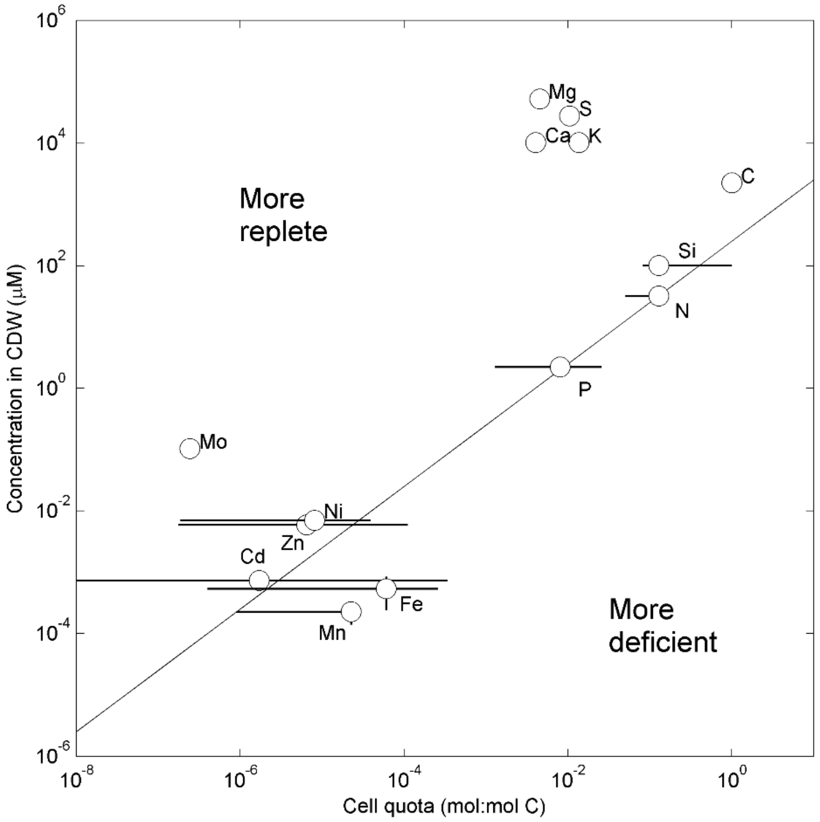
More replete
More deficient
Mg
S
Ca
K
C
Si
N
P
Mo
Ni
Zn
Cd
Fe
Mn
10^{6}
10^{4}
10^{2}
10^{0}
10^{-2}
10^{-4}
10^{-6}
Concentration in CDW (μM)
10^{-8}
10^{-6}
10^{-4}
10^{-2}
10^{0}
Cell quota (mol:mol C)

Figure 1

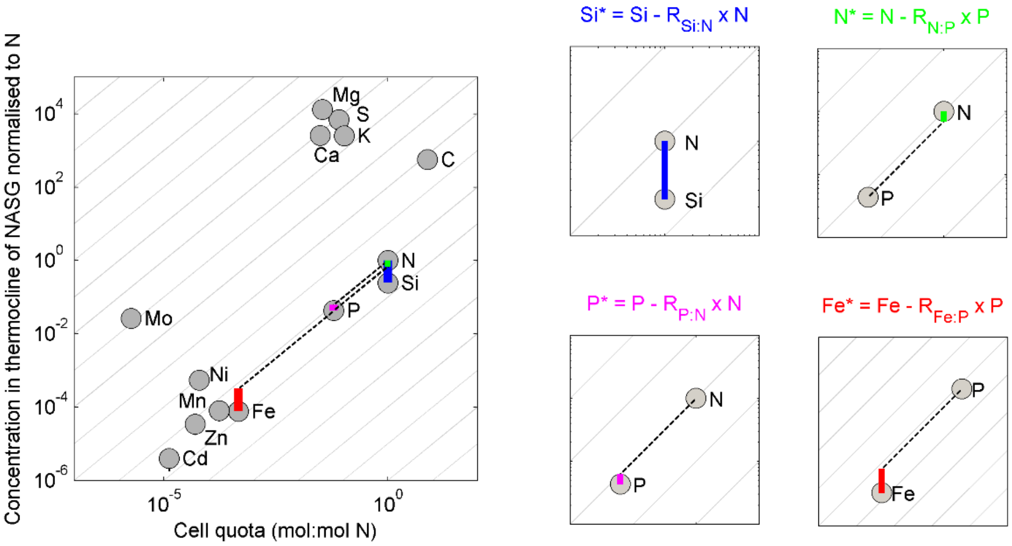
Concentration in thermocline of NASG normalised to N
Cell quota (mol:mol N)
10^{4}
10^{2}
10^{0}
10^{-2}
10^{-4}
10^{-6}
10^{-5}
10^{0}
Mg
S
K
Ca
C
N
Si
P
Mo
Ni
Mn
Fe
Zn
Cd
Si* = Si - $R_{Si:N}$ x N
N* = N - $R_{N:P}$ x P
P* = P - $R_{P:N}$ x N
Fe* = Fe - $R_{Fe:P}$ x P

Figure 2

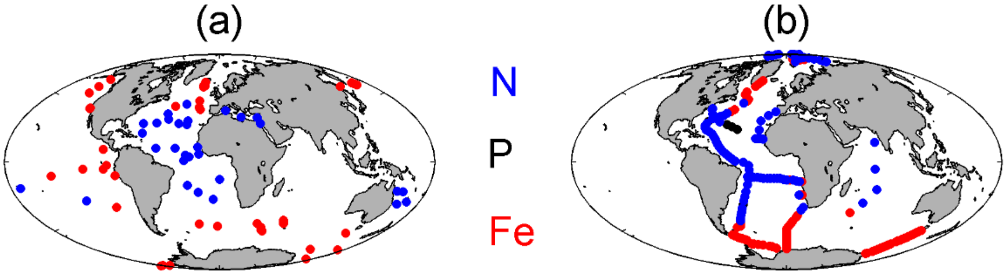

Figure 3

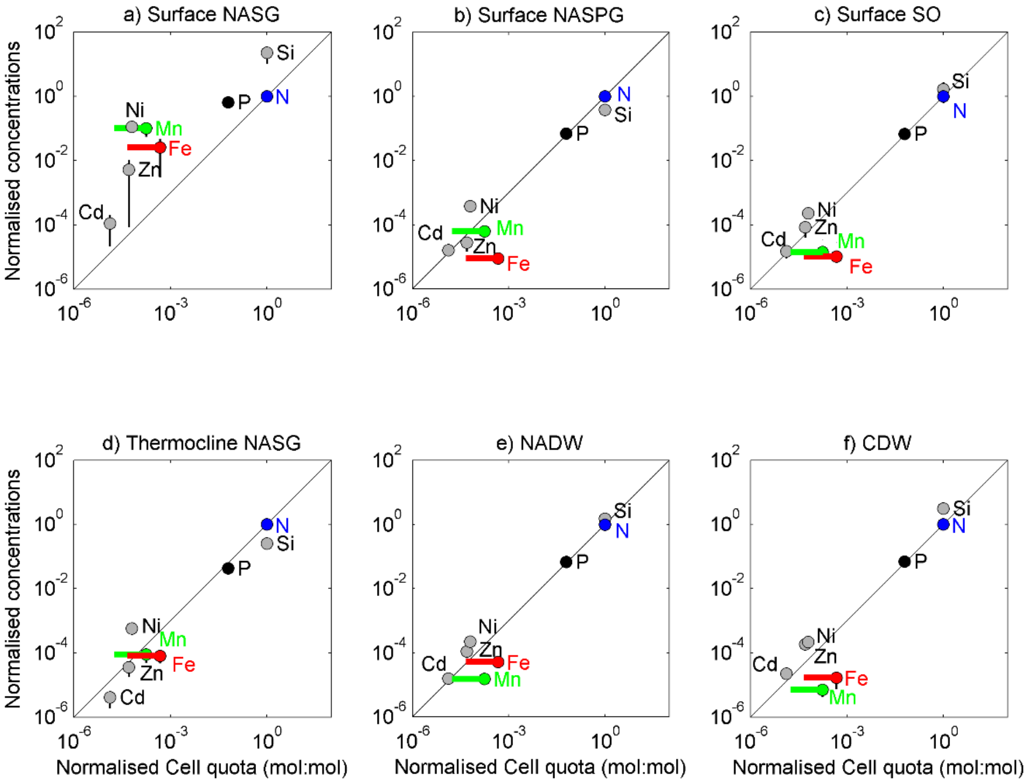
a) Surface NASG
b) Surface NASPG
c) Surface SO
d) Thermocline NASG
e) NADW
f) CDW
Normalised concentrations
Normalised Cell quota (mol:mol)
10^{2}
10^{0}
10^{-2}
10^{-4}
10^{-6}
10^{-3}
Si
N
P
Ni
Mn
Fe
Zn
Cd

Figure 4

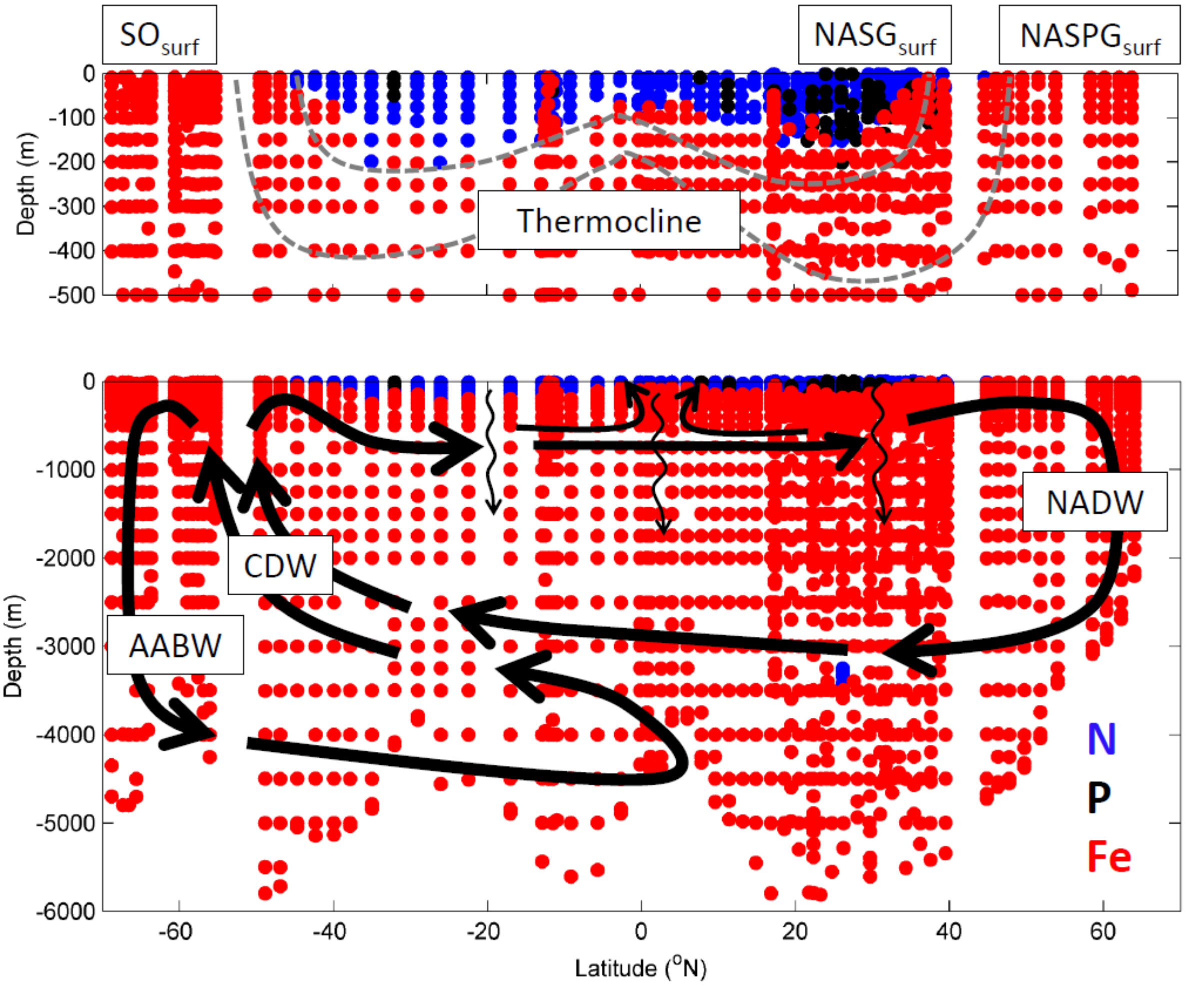
SO$_{surf}$
NASG$_{surf}$
NASPG$_{surf}$
Thermocline
Depth (m)
0
-100
-200
-300
-400
-500
CDW
AABW
NADW
N
P
Fe
0
-1000
-2000
-3000
-4000
-5000
-6000
-60
-40
-20
0
20
40
60
Latitude (°N)

Figure 5

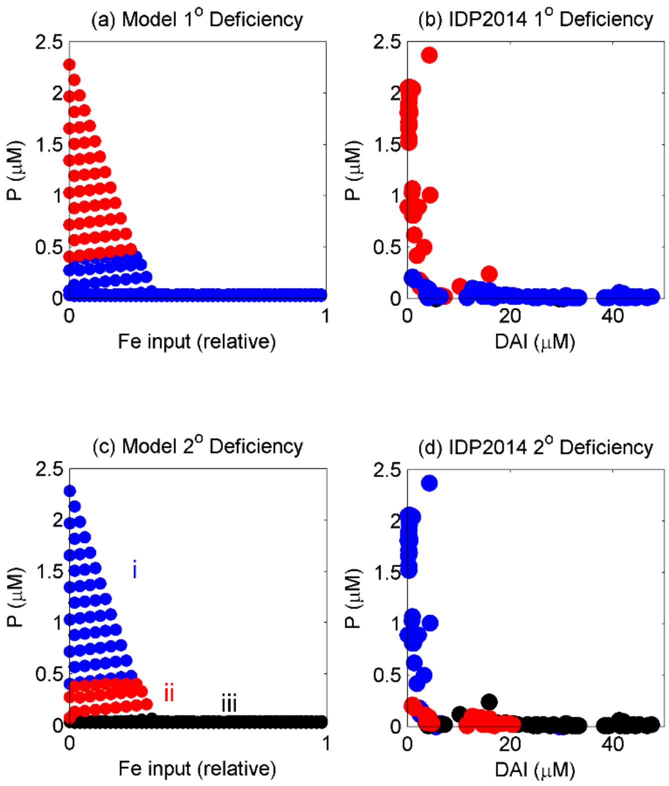
(a) Model 1^o Deficiency
(b) IDP2014 1^o Deficiency
(c) Model 2^o Deficiency
(d) IDP2014 2^o Deficiency
P (µM)
Fe input (relative)
DAI (µM)
2.5
2
1.5
1
0.5
0
0
1
20
40
i
ii
iii

Figure 6

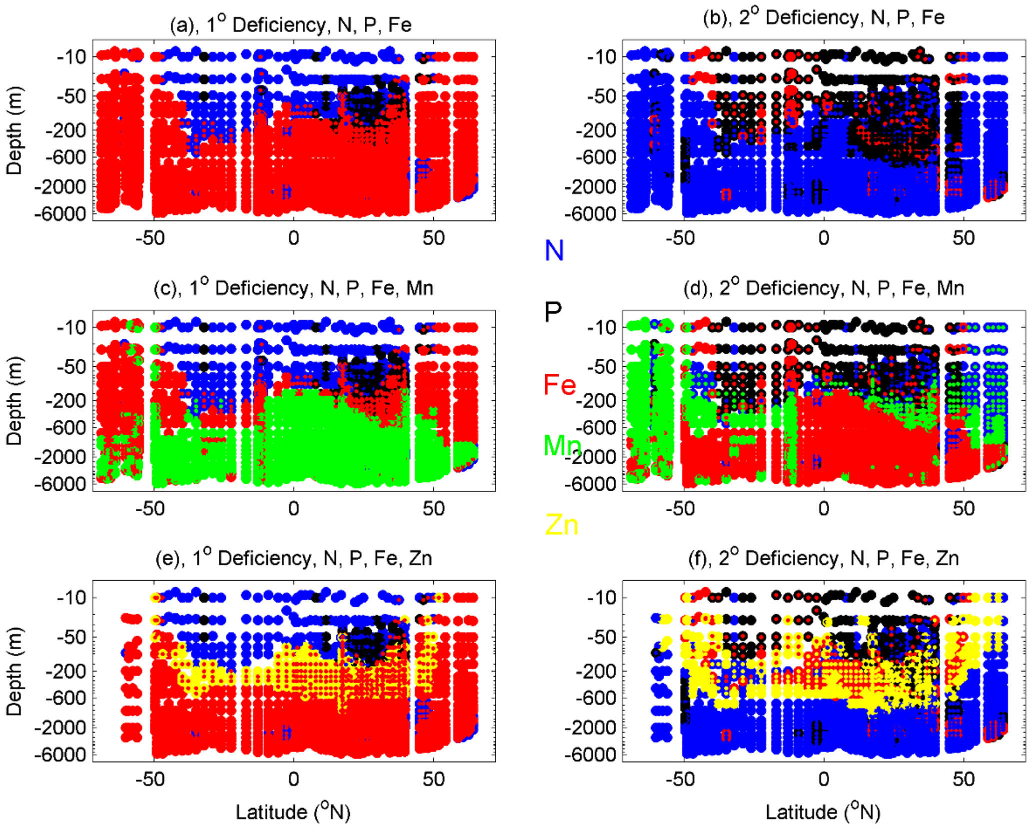
(a), 1^{o} Deficiency, N, P, Fe
(b), 2^{o} Deficiency, N, P, Fe
(c), 1^{o} Deficiency, N, P, Fe, Mn
(d), 2^{o} Deficiency, N, P, Fe, Mn
(e), 1^{o} Deficiency, N, P, Fe, Zn
(f), 2^{o} Deficiency, N, P, Fe, Zn
Depth (m)
-10
-50
-200
-600
-2000
-6000
-50
0
50
Latitude (^{o}N)
N
P
Fe
Mn
Zn

Figure 7